



Colorectal Cancer Disease Classification and Segmentation Using A Novel Deep Learning Approach

M. Siva Naga Raju¹ B. Srinivasa Rao^{1*}

¹*School of Computer Science & Engineering, VIT-AP University, India*

* Corresponding author's Email: msivanaga996@gmail.com

Abstract: In the world, with a death rate of about 35% of colorectal cancer aids as the most widespread type of tumor. The third most commonly diagnosed cancer compared to breast and lung cancer is colorectal cancer. Specifically, in the minimization of health inequalities, it can be supported by the clinical care of AI guidance. Therefore in this paper an effective classification is performed by the deep learning technique called MobileNetV2. Before the classification task, cycle GAN based data augmentation technique is applied to solve the data imbalance problem. Moreover, Mask R-CNN based segmentation is applied to improve the classifier's performance. For the classification of colorectal cancer, the proposed method is examined on a colorectal histopathological dataset (MNIST). The performance of the work will be estimated using precision, accuracy, F-score and recall metrics and the simulation results shows that the proposed classifier achieves 99.91% accuracy, 100% precision, 99.87% recall and 0.999% f1-score over the other state-of-art techniques.

Keywords: Deep learning, Medical image, Cycle GAN, Augmentation, Tissue analysis, R-CNN based segmentation, MobileNetV2 classification.

1. Introduction

Cancer is the uncommon growth of the cell that can attack or disseminate to various parts of the body. Colorectal cancer arises in the colon (large intestine). This cancer is usually seen in aged people and now due to the changes in the lifestyle, it can also be seen in younger people [1-3]. For screening and diagnosing cancer, colonoscopy is the procedure for endoscopy. However, during colonoscopy examination 9-40% of polyps are missed because of its size and type [4-7]. Thus, the performance of current research to maintain an automatic polyp segmentation and classification system promotes endoscopists to detect flat and tiny polyps successfully [8-10].

In examination, medically, a tissue part is removed to be analyzed. It can be used to determine the area of cancer cells as well as the kinds of cancers to which they are linked. Data from microscopy imaging biopsy samples are more complex and greater in size. Computer-assisted diagnostic (CAD)

system's growth in recent years has aided in the decrease of burden. For diagnostic purposes, the biomedical research keeps spreading its energy far and wide [9-11]. Nowadays, to overcome a number of issues in the field of medical image processing deep learning techniques were emerged. Based on CNN for images, a categorization approach of colorectal cancer tissue was presented [12-14].

In existing methods, two datasets are publicly accessible: NCT-CRC-HE-100K and Colorectal Histology based Ensemble Deep Neural Network to Tumor in images of Colorectal Histology, a framework using a classifier of CNN model and a generator of Cycle GAN [14-17]. Mask R-CNN and performance evaluation with different modern convolutional neural networks (CNN) as its feature extractor for polyp segmentation and detection and an ensemble method depending on the dataset of MICCAI polyp detection, (NCT) the National Center for Tumor diseases data sets, to classify the CRC histopathological images, the ResNet-50 model and transfer learning was used. There are some

complexities and failure in few researches in segmentation and accurate image classification [18-20].

To overcome this, segmentation and classification of colorectal cancer is proposed. Initially, to solve the data imbalance problem, cycle GAN based data augmentation is performed. It provides more data for training the sample. The process of generating extra data for training from the existing data is known as data augmentation. Generally, on the input data this is done by using transformations of content preservation by randomly rotating, deforming or image translation. Then, segmentation of image process is carried out with the Modified mask R-CNN. It segments the tissue areas of colorectal cancer. Then, MobileNetV2 based classification is performed to classify the tissue types. MobileNetV2 is similar to MobileNet and it's based on the CNN model that's employed to classify images. The approach uses significantly lower computing power than a standard CNN model and this is the main advantage which is perfect for working over mobiles and the PC's. It works on capabilities of lower computation. A convolution layer is included in the MobileNet model that shift among the accuracy, precision, recall and F-score metrics. The advantages of MobileNet model is, it reduces the size of the network. The dataset used to train the colorectal cancer is Histopathology Colorectal cancer images.

Our contribution toward this work are as follows:

- To design an effective cycle Generative Adversarial Network (cycle GAN) based data augmentation to handle data imbalance problem.
- To design an effective segmentation and classification based on Modified R-CNN and MobileNetV2 model to improve accuracy.

The paper is organized in the following way: The Section 2 presents the works of existing methods. In Section 3 and 4 shows the problem statement and proposed methodology. At last, the result section and conclusion is described in Section 4 and 5.

2. Literature review

The existing work is classified deeply into three subsections handling with the classification, segmentation and augmentation of the procedure in different fields.

Hamida et al. [21] have presented and evaluated state-of-the-art DL models for patch and pixel level classification. For patch level classification task, they used Inception, Densenet, Resnet, Vgg, and Alexnet. For pixel level segmentation, they used segnet and

unet frameworks. However, the computational cost of segmentation method (Segnet) is too high and it produce more false positives. To balance the classes of tumor and non tumor images, the authors introduced weighted cross entropy loss method.

Deep neural network (DNN) based colorectal cancer classification and segmentation was conducted by Ghosh et al. [22]. For this purpose, three various DNN architectures were combined to create the Ensemble DNN and performed the classification and segmentation task. But it take more time and space for training and testing due to its architecture. To evaluate the performance of the technique, the colorectal histology data from two standard dataset were utilized.

For colorectal cancer tissue classification, a CNN based frameworks and various machine learning techniques were suggested by Ohata et al. [23]. For deep feature extraction, the transfer learning based various CNNs such as inception, VGG, Densenet etc. were utilized. Based on these extracted features several machine learning classifiers were implemented. Finally, the authors selected the best feature extractor and classifier combination based on their performance on tissue classification (densenet and SVM). The computation cost and performance of this approach is good but the accuracy rate of this approach is very poor compared to our proposed technique.

Tsai and Tao [24] suggested five deep learning based architectures for colon tissue classification such as Alexnet, GoogleNet, Squeezenet, VGGNet, and Resnet. The authors used transfer learning based deep learning architecture to improve the performance of the classifier. Finally, they concluded that the resnet achieved best performance. But the architecture of this network is highly complex and the number of samples in the dataset are unbalanced.

The pixel level classification of Colon cancer based on VGG-16 network was implemented by Damklian et al. [25]. For data augmentation, RGB re-scaling technique was applied. To initialize the learning rate parameter, Adam optimizer was utilized. But the training time of this network is too long and it is computationally expensive.

3. Problem statement

For colorectal polyps, methods of deep learning for classification & segmentation are developed based on the aforesaid examination of literature on optical colorectal images and colonic pathology. The data imbalance problem occurs when the number of samples in each class varies. The model may be overfitted because of the large number of images in

many classes. Training and defining an architecture for segmentation from the beginning isn't an easy task. To retrieve the images of colonoscopy, the training procedure usually necessitates a massive proportion of images and that is challenging. Colorectal optical pictures might be difficult to diagnose. The interference of liquid and low light often result in colorectal images bad imaging superiority. And, the edges of normal tissues/polyps are unclear. Due to this, the normal and polyp tissue's classification accuracy is to be reduced and the sorts of polyps and margins of normal tissue are convoluted. It causes the classification accuracy of, polyp and normal tissue to be low. To overcome these issues, the proposed method is used for the better performance for this research.

4. Proposed methodology

The conceptual framework of our proposed method is to design an effective cycle Generative Adversarial Network (cycle GAN) based data augmentation to handle data imbalance problem. By using the Cycle GAN technique, each classes training data with minimum images can be augmented with more images. To design an effective segmentation, a modified R-CNN for polyp segmentation is proposed in this paper. To segment the obtained images after data augmentation, R-CNN is implemented for the polyp segmentation. In addition, MobileNetV2 for classification is proposed in this research work. The model requires less computing effort than the conventional model which is the advantages of using the architecture of MobileNet. The MobileNet model also reduces the network size and it is also considered as one of the advantages. To analyze the effectiveness of proposed approach, the following parameters are considered: Accuracy, Precision, Recall, F-score. The notations used in this paper and the overall architecture is shown in Table 1 and Fig. 1.

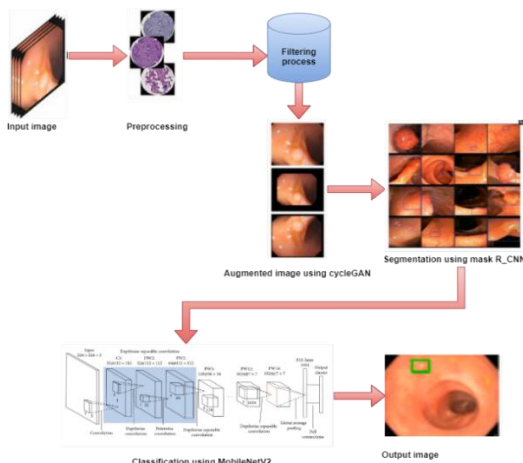


Figure. 1 Architecture diagram of proposed methodology

Table 1. Notation details

Notation	Definition
I	Reference domain
J	Target domain
p_d	Data Samples
D	Discriminator
G	Generator
L	Loss
A	Anchor
B	Encoding box
l_{cls}	Classification loss
f_{loc}	Location based loss
f_{mask}	mask loss
m	mini-batch size
N	anchors number
F_s	Filter of size
F_m	Feature vector size
P	input
Q	Output
C_e	actual computing performance
$cost_e$	Computation cost

4.1 Data pre-processing

Initially, to remove any further noise of image, the input image has been pre-processed. In an image, the entire quality of the image will be affected by the additional noise. By performing the pre-processing step, for enhancing the quality of the image and to acquire better image quality of image processing. The input images are pre-processed after the image acquisition. Basically, image pre-processing is used to efficiently remove noise in the input image and to rectify the image's blurred area. From the gathered images for obtaining clearer and much improved data the effect of tinkling effect is used.

4.2 Data filtering

During this process, a high-pass filter is applied. For the purpose of medical research, the method employs the use of required samples of images. For a high-quality image, the high-pass filter is dependent on a mask and the sobel operator is employed. For obtaining the improved image quality, filtering treatment of grayscale image is developed. In deep Learning "filters" refers to the convolutions trained weights. A single 3x3 convolution is called a "filter" and it has a total of 10 weights. In data filtering, the removal of colorectal images of blurry occurs.

The endoscopic image combination of healthy tissue, tumour and polyp are captured after the

process of image filtering under either narrow band imaging (NBI) or white light (WL) endoscopy. Filtering the images before the convolution process is done mainly to obtain the clear images.

4.3 Cycle GAN overview

Cycle GAN comprises of two generators and two discriminators. If suppose, A and B are different classes. G_{ab} is a generator that changes A's domain to B's, and D_b is a discriminator which distinguishes among real data from classes A and B and the data that was acquired with G_{ab} . Such that, G_{ab} & D_b are combative networks, the loss can be represented as follows:

$$L_{a \rightarrow b} = E_b[\log D_b(B)] + E_b[\log(1 - D_b(G_{ab}(a)))] \quad (1)$$

Similarly, the generator loss, G_{ba} which converts domain of B to that of A and the discriminator D_a also expressed as equation:

$$L_{b \rightarrow a} = E_a[\log D_a(A)] + E_b[\log(1 - D_a(G_{ba}(b)))] \quad (2)$$

Thus, Cycle GAN has eased this mode collapse issues by modelling cycle consistency loss, L_{cyc} , so to reconstruct it can only change as that it could.

$$L_{cyc} = E_a[\|G_{ba}(G_{ab}(a)) - a\| + E_b[\|G_{ab}(G_{ba}(b)) - b\|]] \quad (3)$$

4.4 Data augmentation using CGAN

Cycle GAN (cycle Generative adversarial network) is used to increase the training set of images to overcome the data imbalance problem. Cycle GAN is proposed for image-to-image change, based on CNN. For increasing the images of augmented data, for each case the generator of colorectal cancer transformation are trained. We always observe a chance of overfitting, when using CNN with many layers or handling with inadequate training specimen. Imbalanced data problem is continuously based on misclassification. Data augmentation is the standard solution to decrease misclassification and overfitting, it enhances the results of classification in which it artificially magnifies and balances the dataset.

The data can be augmented in two paths: 1) Random rotation, shear, flips and shifts etc. which is said to be the classical process 2) Using generative modelling for generating samples trained from the related data. On using Generative Adversarial

Networks (GANs), method of generating synthetic images of colorectal cancer diseases is elaborated. These techniques are applied to our Colorectal histopathology images dataset (MNIST). Cycle GAN trains a generator that generates images in one domain. Many possible viable mappings can be done without the use of pairing information. These models are trained with a constraint of cycle-consistency in order to reduce the space of viable mappings. To generate artificial colorectal cancer disease images, Cycle GAN technique uses both loss of cycle-consistency and adversarial networks. The two domains I and J is given, the mapping among the elements of two domains viably many-to-many occurs. Probably, the goal is to use unpaired samples from each domain distributions $p_d(i)$ and $p_d(j)$ Here, the samples are denoted by p_d . On using the samples from the true marginal, we try to calculate the true condition $p(i|j)$ and $p(j|i)$. A major hypothesis is that the items in domains I and J are highly correlated without any information of pairing. This model deals with the mappings such as $G_{IJ}: I \rightarrow J$ and $G_{JI}: J \rightarrow I$, parameterized by DCNN. It accepts some of the constraints a) Each mapping's output relates to the distribution of the target domain, on concentrating the source domain and this is said to be as the process of marginal matching. b) Mapping the elements among each other, and then again mapping back, should get the source domain that we began at first.

The constraint of the first is accepted using GAN. Mappings G_{IJ} and G_{JI} are represented by DNN which are trained to trick the adversarial discriminators such as D_I and D_J . On applying this matching to the target domain, J is degraded over the source domain I , regarding to G_{IJ} :

$$L_{GAN}^I(G_{IJ}, D_J) = E_{i \sim p_d(i)} [ij D_J(i) + E_{g \sim p_d(j)} [ij (1 - D_I(G_{IJ}(j)))] \quad (4)$$

Then to increase the adversarial objective is trained by D_J . In the opposite direction, a parallel adversarial $L_{GAN}^J(G_{JI}, D_I)$ is settled for matching marginally. The objective is enforced by the cyclic consistency starting a sample i from I , the j is reconstructed and it is given by, $j = G_{JI}(G_{IJ}(i))$ which is as closer to i . Relationship between j and j' is calculated with L1 or L2. On utilizing the L1 norm, cycle-consistency which starts from I is calculated as:

$$L_{CYC}^J(G_{JI}, G_{IJ}) = E_{j \sim p_d(j)} \|G_{JI}(G_{IJ}(j)) - j\| \quad (5)$$

Thus, for cycle-consistency which starts from J , the whole objective is given by:

$$L_{GAN}^I(G_{JI}, G_{IJ}) + L_{GAN}^J(G_{IJ}, D_J) + \alpha L_{CYC}^A(G_{IJ}, G_{JI}) + \alpha L_{CYC}^J(G_{IJ}, G_{JI}) \quad (6)$$

Where, α is a hyper-parameter (weight) to stabilize marginal matching and cycle-consistency. Marginal matching encourages the generation of realistic samples in any one of the domains.

To capture high-level concepts and features DNN is proposed in Cycle GAN. The quality convergence and convergence rate are affected by the vanishing gradient problem. A patch-based discriminator D and G is utilized and trained together. A filter size of 4×4 is used by all the convolutional layers in D . This novelty of the generator of cycle GAN and discriminator of Patch-wise architecture enables effectual training and improves convergence quality.

4.5 Data segmentation

R-CNN for mask is a general background and it is an advancement of Faster R-CNN. The framework for Mask R-CNN is shown in Fig. 2. The beginning stage of R-CNN is said to be the region proposal network and it is adjusted by mask R-CNN. It appends a fresh branch to the next stage for the prediction of parallel object mask. To fix the problem of misalignment, RoIAlign is used by mask R-CNN, and the layer of free quantization is used for polyp detection and segmentation. CNN based feature extractors of varying type is used to calculate the Mask R-CNN performance. A multiple loss of task on every area of interest known as anchor and is presented by RPN (Region proposal network) is used to train the model. For each anchor 'a', the matching ground-truth box 'b' is found. Then, behaves as a positive anchor if there is a matching among 'a' and 'b' and the class label is assigned as $y_a = 1$, and $(\varphi(b_a; a))$ encoding box 'b' is assigned. Anchor 'a' behaves as a negative, if there is a mismatch between anchor 'a' and 'b', the class label is assigned as $y_a = 0$. For per anchor, the mask branch is of 14×14 -dimension output. The anchor 'a' loss consists of three losses: (1) Classification loss 'cls' for the detected class $l_{cls}(I; a, \theta)$, (2) location-based loss 'loc' for the anticipated box $f_{loc}(I; a, \theta)$ and (3) mask loss for the anticipated mask $f_{mask}(I, a, \theta)$: where I is said to be the image and θ is denoted as the parameter,

$$L(a, I; \theta) = \frac{1}{m} \sum_{i=1}^m \frac{1}{N} \sum_{j=1}^N 1[a \text{ is positive}] \cdot \ell_{loc}(\Phi(b_a; a) - f_{loc}(I; a, \theta)) + l_{cls}(y_a, f_{cls}(I; a, \theta)) + l_{mask}(mask_a, f_{mask}(I, a, \theta)) \quad (7)$$

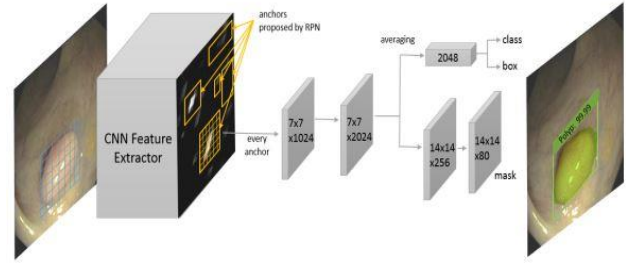


Figure. 2 Framework of mask R-CNN

Where, m is the mini-batch size and for every frame N is the anchors number. Thus, the following functions of loss is used: (1) Softmax for the loss of classification (2) Smooth L1 for the loss of localization (3) binary cross-entropy for mask loss.

4.6 Deep learning based MobileNetV2 for classification

To classify the images, MobileNet V2 which is the extension of MobileNet. This approach is depending on CNN. Among mobile device,s it is appropriate for functioning and the PC's, they operate on computers with limited computation power. The model of MobileNet is a more straightforward framework that relies on the accuracy, precision, recall and F-score of metrics prominently. With a small subset of properties, this framework is highly effective. The basic structure is based on various layers of abstraction and the MobileNet architecture is depth-wise. The 1×1 is known as difficulty of point-wise. Systems for in-depth creation usually established with levels of abstraction with standard (ReLU). The filter of size $F_s \times F_s$ and the feature vector map of size $F_m \times F_m$ and p stands for the variable of input, while q stands for the variable of output. The variable C_e indicates the actual computing performance in terms of design and can be assessed using the equation below (7):

$$C_e = F_s \cdot F_s \cdot \omega \cdot \alpha F_m + \omega \cdot \rho \cdot \alpha F_m \cdot \alpha F_m \quad (10)$$

Multiplication has a situation-dependent value and in the range of 1 to n, the multiplier value ω is assigned for the experimental evaluation.

The ' α ' value is considered to be 1, where α is the variable resolution multiplier. The efforts of computation can be recognized by the variable $cost_e$ and can be evaluated by the mathematical expression (8):

$$cost_e = F_s \cdot F_s \cdot \omega \cdot \rho \cdot F_m \cdot F_m \quad (11)$$

The proposed model involves the point-wise and depth-wise convolutions, then it is limited by the

depletion variable 'd' and it is represented by the Eq. (9):

$$d = \frac{F_s \cdot F_s \cdot \omega \cdot \alpha F_m \cdot \alpha F_m + \omega \cdot \rho \cdot \alpha F_m \cdot \alpha F_m}{F_s \cdot F_s \cdot \omega \cdot \rho \cdot F_m \cdot F_m} \quad (12)$$

The layers of an Advanced Residual Mobile NetV2 (CNN) approach are selected, compare with other methods for the classification of images, CNNs contain limited pre-processing measures.

The next step to a convolution layer is a simple straightforward layer of units. The process has been described using feature charts to enhance the network's nonlinear behavior. Values of negative are rapidly removed in this case.

a) Convolution layer

To focus on data of the images is the main reason of this layer. In the input image, this method recognizes the functions as well as provides the mapping functions.

b) Pooling layer

The input scale eventually decreases as the pooling cycle continues. Overfitting is eliminated during the process of pooling. The appropriate settings are shown as the parameter's number increases.

c) Flattening layer

In the analytics of consecutive column with flattening the pooling layer map, it is truly a simple move.

d) Fully connected layer

The characteristics are associated with the properties in this layer. The classification process is finalized with the inaccuracy of massive percentage. Primarily, the error is noted and monitored.

e) Softmax

The softmax is applied for predicting the output classes' probability distribution in neural grids to map unregulated operation of the network. The Softmax has been used for analysis of many issues in a variety of domains. The Decimal chance is like 1.0.

ALGORITHM FOR MOBILENETV2 CLASSIFICATION

Input: Improved image

Output: filtered image

Begin from the network layer

Begin from features trained

Begin to label

Training Label =70%

Testing Label =30%

Lab=One (label)

For ii=1: (length (Lab))

Class= Calculate (label== Lab (ii))

Train cut=length (class)-traincut

Train data=[data training; features training;

class (1: Train cut)]

Assume labels=classify (net, train data)

Stop

For ii=1: size (datatrain,1)

Train data = [data training; features training;

class (1: Train cut)]

Stop

For ii=1: size (trainfeatures,1)

Data Training= [features training; features training;

class (1: Train cut)]

Stop

5. Simulation results

This section explores the developed system's performance on Colorectal Histology dataset(MNIST) (5000 images). The models have been trained using the MNIST dataset, with 625 images among 5000 images for each class such as Empty, Adipose, Mucosa, Debris, Lympho, Complex, Stroma and Tumor. From the dataset, 80% data are splitted into training set and remaining 20% are in test set. The proposed technique is trained and tested on Windows 10 operating system with Anaconda navigator and 16 GB of RAM. All the simulations are performed on Keras with Tensorflow at the backend. After the training process, the method is evaluated on testing data based on the performance metrics like Accuracy, precision, recall and F1-score.

$$accuracy = \frac{TP+TN}{TP+FP+TN+FN} \quad (13)$$

$$recall = \frac{TP}{TP+FN} \quad (14)$$

$$precision = \frac{TP}{TP+FP} \quad (15)$$

$$f1 - score = 2 \times \frac{precision \times recall}{precision + recall} \quad (16)$$

Here, the TP, TN, FP, FN denotes the true positive, true negative, false positive, false negative respectively.

5.1 Data augmentation results:

Fig. 3 signifies the unbalanced and balanced data-based data augmentation using cycleGAN in order to overcome the imbalance problem of colorectal cancer using MNIST dataset for eight classes. Once after the augmentation is done for eight classes the images are

generated. In addition, eight images is generated for cycle GAN from input images for each eight classes and eight images is generated for histogram equalized images. For eight input images classes totally 16 images are generated from the histopathology colorectal cancer dataset. The validation set loss is comparatively high on relating to the training set, when the model of Cycle GAN is trained by the utilization of original training data. The results of training after the process of data augmentation indicates that the set of validation loss is decreased nearer to the set of training level. An unbalanced and balanced dataset for existing and proposed cycle GAN is shown below in Table 2.

The performance evaluation among the unbalanced and balanced dataset is shown as a graph in Fig. 3 and the augmentation using cycle GANs for each class is shown in Fig. 4.

The model’s capability is determined by the proposed MobileNetV2 performance which is calculated through the hyperparameters. In this model’s training rate at various levels is described in this section. The performance evaluation in terms of F-score, recall, precision, and accuracy are presented on comparing with existing methods and it is represented in Table 3.

Table 2. Performance evaluation for eight classes in colorectal cancer to handle imbalance problem

Classes	Unbalanced cycle GAN	Balanced cycle GAN using MNIST dataset
Empty	1.900	7.500
Adipose	7.940	7.950
Mucosa	8.125	8.125
Debris	8.000	6.100
Lympho	1.910	8.000
Complex	1.956	6.120
Stroma	1.806	4.580
Tumor	1.806	8.000

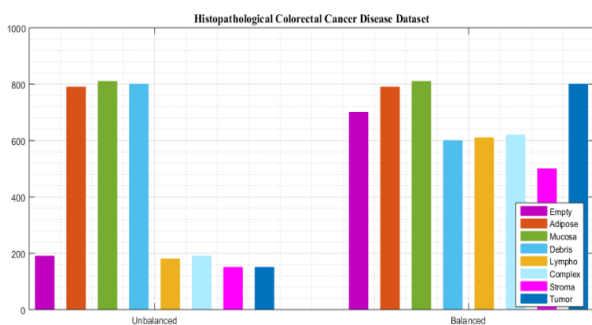


Figure. 3 Comparison of unbalanced and balanced data-based data

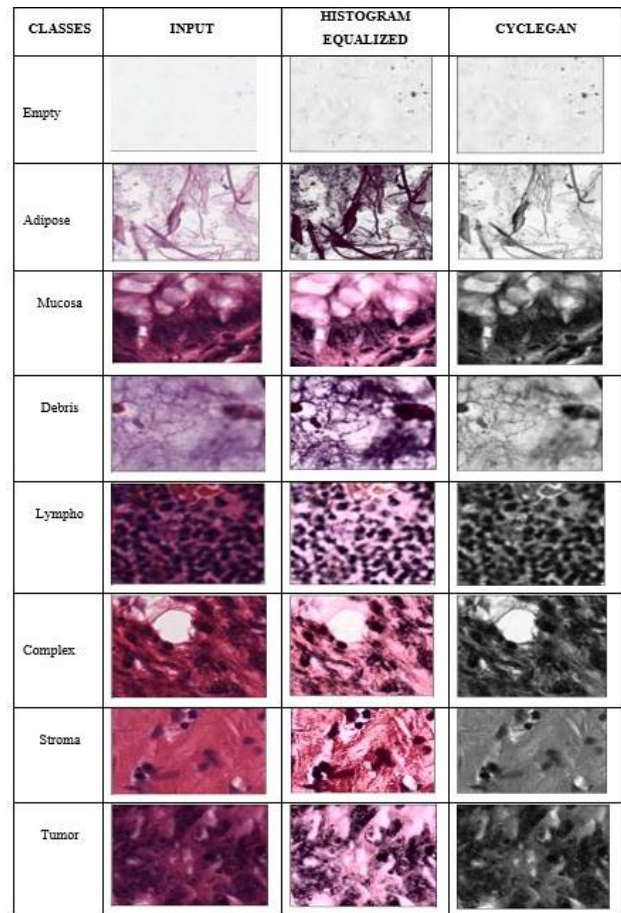


Figure. 4 Augmentation using cycle GANs for each class

From the Table 3, it is observed that the proposed CycleGAN-MobileNetV2 model obviously outperforms existing models. The existing technique VGG-16 and Segnet techniques achieves good results but the Segnet provides more false positive values. Moreover the training time of VGG-16 is too long. Compared to Densenet169-SVM, the performance of ResNet50 is better but it is lower than other techniques. The Accuracy comparison of proposed with existing techniques are represented in Fig. 5.

Table 3. Comparative analysis of existing and proposed method classification

Models	Accuracy	Precision	Recal l	F-score
SegNet [21]	98.66	-	98.14	-
Ensemble DNN [22]	92.83	92.83	93.11	92.97
Densenet169+ SVM [23]	92.8	-	-	92.12
ResNet50 [24]	94.86	-	-	-
VGG-16 [25]	97.6	95.3	95	96
Proposed CycleGAN+ MobileNetV2	99.91	100.00	99.87	99.9

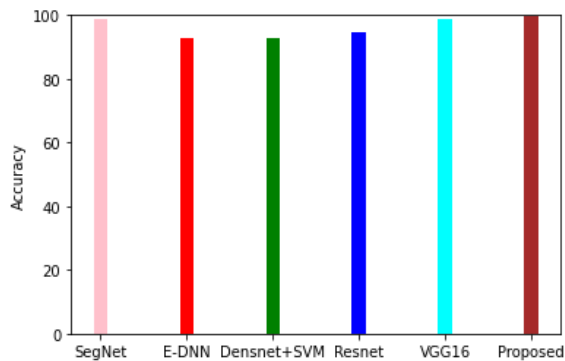


Figure. 5 Graphical representation for accuracy among existing and proposed method

In terms of F-score, Ensemble DNN and Densenet achieves similar results. Moreover, the VGG-16 technique attains good results (96%) than the other techniques. When compared to segnet, the recall value of VGG-16 is lower. Then comparing the overall performance, the proposed approach achieves superior performance in all metrics (Accuracy 99.91%, Precision 100%, recall 99.87% and f1-score 99.9%)

Fig. 6 shows the diagrammatic representation using modified RCNN. The designed methodology, according to the evaluation, is superior when related to prevailing one. The final detected image is obtained using MobileNetV2 classification and is shown in Fig. 7.

Finally, based on the above evaluation, it is concluded that the performance of the proposed approach is superior to the other techniques in terms of 99.91% accuracy.

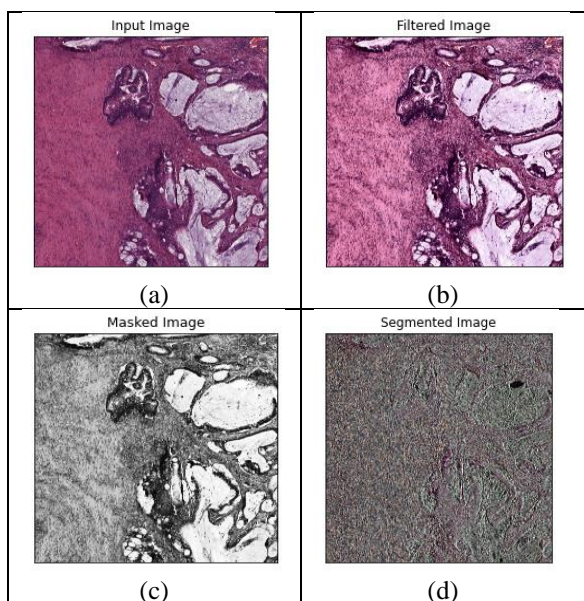


Figure. 6 Representation of: (a) Input image, (b) Filtered image, (c) Masked image, and (d) Segmented image using modified RCNN

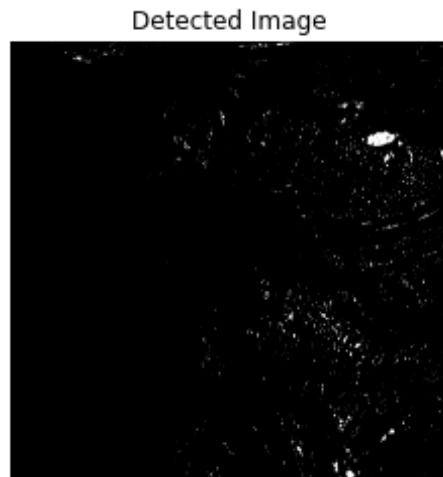


Figure. 7 Final output image

6. Conclusion

In this paper, segmentation and classification of colorectal cancer are proposed. Initially, to solve the data imbalance problem, cycle GAN based data augmentation is performed. It provides more data for the training sample. Afterward, the image segmentation process is carried out with the Modified mask R-CNN. It segments the tissue areas of colorectal cancer. Then, MobileNetV2 based classification is performed to classify the tissue types. The simulation of the proposed approach is implemented by using TensorFlow. Moreover, the performance of the proposed approach is evaluated based on the performance metrics named Accuracy, Precision, Recall, and F-score and compared with other state of art techniques. The images are given as input, then the images are preprocessed, filtered, segmented and the final output is obtained. In the future, with regards to colorectal polyp segmentation, the enhanced algorithm of classification and standard data of quality will be incorporated. On exploring Mask R-CNN, other backbone structures can be used for the segmentation process. Moreover, a high-quality colorectal polyp’s dataset of huge amounts can be generated and uniquely classified.

Conflict of interests

We declare that this manuscript is original, has not been published before and is not currently being considered for publication elsewhere.

Author Contributions

M. Siva Naga Raju contributed to methodology and implementation, writing review, B Srinivasa Rao contributed in supervising the overall work and editing the paper.

References

- [1] Y. Yao, S. Gou, R. Tian, X. Zhang, and S. He, "Automated Classification and Segmentation in Colorectal Images Based on Self-Paced Transfer Network", *BioMed Research International*, 2021.
- [2] E. Paladini, V. Edoardo, B. Fares, D. Cosimo, H. Abdenour, and T. Abdelmalik, "Two Ensemble-CNN Approaches for Colorectal Cancer Tissue Type Classification", *Journal of Imaging*, Vol. 7, No. 3, p. 51, 2021.
- [3] T. D. Bel, B. J. Melle, L. J. V. Der, and L. Geert, "Residual cyclegan for robust domain transformation of histopathological tissue slides", *Medical Image Analysis*, Vol. 70, p. 102004, 2021.
- [4] J. N. Kather, K. Johannes, C. Pornpimol, L. Tom, H. Esther, W. C. Aron, G. Timo, and N. Halama, "Predicting survival from colorectal cancer histology slides using deep learning: A retrospective multicenter study", *PLoS Medicine* Vol. 16, No. 1, p. e1002730, 2019.
- [5] O. J. Skrede, S. D. Raedt, A. Kleppe, T. S. Hveem, K. Liestøl, J. Maddison, and H. E. Danielsen, "Deep learning for prediction of colorectal cancer outcome: a discovery and validation study", *The Lancet*, Vol. 395, No. 10221, pp. 350-360, 2020.
- [6] E. Vorontsov, M. Cerny, P. Régner, P. L. D. Jorio, C. J. Pal, R. Lapointe, and A. Tang, "Deep learning for automated segmentation of liver lesions at CT in patients with colorectal cancer liver metastases", *Radiology: Artificial Intelligence*, Vol. 1, No. 2, p. 180014, 2019.
- [7] D. Bychkov, L. Nina, T. Riku, N. Stig, E. K. Panu, V. Clare, W. Margarita, L. Mikael, H. Caj, and L. Johan, "Deep learning-based tissue analysis predicts outcome in colorectal cancer", *Scientific Reports*, Vol. 8, No. 1, pp. 1-11, 2018.
- [8] N. Ito, H. Kawahira, H. Nakashima, M. Uesato, H. Miyauchi, and H. Matsubara, "Endoscopic diagnostic support system for cT1b colorectal cancer using deep learning", *Oncology*, Vol. 96, No. 1, pp. 44-50, 2019.
- [9] T. Binder, E. M. Tantaoui, P. Pati, R. Catena, A. S. Aghayan, and M. Gabrani, "Multi-organ gland segmentation using deep learning", *Frontiers in Medicine*, Vol. 6, p. 173, 2019.
- [10] X. Wu, Y. Li, X. Chen, Y. Huang, L. He, K. Zhao, and Z. Liu, "Deep learning features improve the performance of a radiomics signature for predicting KRAS status in patients with colorectal cancer", *Academic Radiology*, Vol. 27, No. 11, pp. e254-e262, 2020.
- [11] M. M. Abdelsamea, A. Pitiot, R. B. Grineviciute, J. Besusparis, A. Laurinavicius, and M. Ilyas, "A cascade-learning approach for automated segmentation of tumour epithelium in colorectal cancer", *Expert Systems with Applications*, Vol. 118, pp. 539-552, 2019.
- [12] D. Sarwinda, P. RadifaHilya, B. Alhadi, and A. Pinkie, "Deep learning in image classification using residual network (ResNet) variants for detection of colorectal cancer", *Procedia Computer Science*, Vol. 179, pp. 423-431, 2021.
- [13] N. Dif and E. Zakaria, "A new deep learning model selection method for colorectal cancer classification", *International Journal of Swarm Intelligence Research*, Vol. 11, No. 3, pp. 72-88, 2020.
- [14] M. Shaban, A. Ruqayya, F. M. Moazam, A. Ayesha, T. Y. Wah, S. David, and R. Nasir, "Context-aware convolutional neural network for grading of colorectal cancer histology images", *IEEE Transactions on Medical Imaging*, Vol. 39, No. 7, pp. 2395-2405, 2020.
- [15] Y. Zhou, G. Simon, K. Navid, S. Muhammad, H. P. Ann, and R. Nasir, "Cgc-net: Cell graph convolutional network for grading of colorectal cancer histology images", In: *Proc. of the IEEE/CVF International Conference on Computer Vision Workshop*, 2019.
- [16] J. Ronen, H. Sikander, and A. Altuna, "Evaluation of colorectal cancer subtypes and cell lines using deep learning", *Life Science Alliance*, Vol. 2, No. 6, 2019.
- [17] K. He, L. Xiaoming, L. Mingyang, L. Xueyan, Y. Hualin, and Z. Huimao, "Noninvasive KRAS mutation estimation in colorectal cancer using a deep learning method based on CT imaging", *BMC Medical Imaging* Vol. 20, No. 1, pp. 1-9, 2020.
- [18] X. Yue, D. Neofytos, and A. Ognjen, "Colorectal cancer outcome prediction from H&E whole slide images using machine learning and automatically inferred phenotype profiles", *arXiv Preprint*, 2019.
- [19] K. Damkliang, W. Thakerng, and T. Paramee, "Tissue classification for colorectal cancer utilizing techniques of deep learning and machine learning", *Biomedical Engineering: Applications, Basis and Communications*, Vol. 33, No. 03, 2021.
- [20] S. Vidhya and R. Shijitha, "Deep Learning based Approach for Efficient Segmentation and Classification using VGGNet 16 for Tissue Analysis to Predict Colorectal Cancer", *Annals of the Romanian Society for Cell Biology*, pp. 4002-4013, 2021.

- [21] A. B. Hamida, M. Devanne, J. Weber, C. Truntzer, V. Derangère, F. Ghiringhelli, and C. Wemmert, “Deep learning for colon cancer histopathological images analysis”, *Computers in Biology and Medicine*, Vol. 136, p. 104730, 2021.
- [22] S. Ghosh, B. Ahana, S. Shreya, G. Richik, K. Ishita, and K. C. Santosh, “Colorectal histology tumor detection using ensemble deep neural network”, *Engineering Applications of Artificial Intelligence*, Vol. 100, p. 104202, 2021.
- [23] E. F. Ohata, C. J. V. S. Das, B. G. Maia, H. M. Mehedi, and V. H. C. Albuquerque, “A novel transfer learning approach for the classification of histological images of colorectal cancer”, *The Journal of Supercomputing*, Vol. 77, No. 9, pp. 9494-9519, 2021.
- [24] M. J. Tsai and Y. H. Tao, “Deep Learning Techniques for the Classification of Colorectal Cancer Tissue”, *Electronics*, 10(14), 1662, 2021.
- [25] K. Damkliang, W. Thakerng, and T. Paramee, “Tissue classification for colorectal cancer utilizing techniques of deep learning and machine learning”, *Biomedical Engineering: Applications, Basis and Communications*, Vol. 33, No. 03, p. 2150022, 2021.